Materials Letters 125 (2014) 111–115

Contents lists available at ScienceDirect

Materials Letters

journal homepage: www.elsevier.com/locate/matlet

Facile preparation of hydroxyapatite–chondroitin sulfate hybrid mesoporous microrods for controlled and sustained release of antitumor drugs

Yuming Guo *, Xiaoman Shi, Qilong Fang, Jie Zhang, Hui Fang, Weili Jia, Gai Yang, Lin Yang *

School of Chemistry and Chemical Engineering, Henan Normal University, Xinxiang 453007, PR China

ARTICLE INFO

Article history:
Received 8 October 2013
Accepted 15 March 2014
Available online 21 March 2014

Keywords:
Hydroxyapatite
Mesoporous microrods
Microstructure
Controlled release
Biomaterials

ABSTRACT

In the present study, using chondroitin sulfate as morphology-directing matrix, hydroxyapatite–chondroitin sulfate hybrid mesoporous microrods were prepared successfully through a facile one-pot method under mild conditions. From the results, the antitumor drug doxorubicin hydrochloride (DOX · HCl) could be loaded into the as-prepared microrods efficiently owing to the large specific surface area and the presence of the mesopores. In addition, the loaded DOX · HCl could be controlled released with pH-dependent and sustained features. These suggest that the hybrid mesoporous microrods prepared in this study might be used as the potential targeted drug delivery carrier to treat the human tumors clinically with good specificity and long duration.

1. Introduction

Currently, the treatment effectiveness of the chemotherapeutic drugs is limited because of the poor tumor specificity and the severe side effects [1]. Considering the advantages of drug delivery systems (DDS) over pure drugs, nowadays, DDS have attracted tremendous attention [2,3]. Recently, the targeted DDS modified with recognition agents has come into the focus of attention [4–6]. However, hitherto, most of the targeted DDS are polymer-based and the applications are seriously limited by the sophisticated preparation and safety concerns [7,8]. Owing to the advantages of inorganic materials over polymers, including facile preparation and non-involvement of toxic reagents, these materials might be the good candidates for DDS [9,10]. For example, the potential application of the porous SiO_2 as DDS has been intensively studied recently [11,12]. Because of the superiority of calcium-based materials over SiO_2, such as the better biocompatibility, biodegradability and pH sensitivity [13–15], the preparation and application of the calcium-based targeted DDS have attracted our attention.

Herein, hydroxyapatite–chondroitin sulfate hybrid mesoporous microrods (HAP–CSMRs) were prepared through a one-pot strategy. From the results, the antitumor drug doxorubicin hydrochloride (DOX · HCl) could be loaded into HAP–CSMRs efficiently owing to the large specific surface area (SSA) and mesopores. In addition, the DOX · HCl could be controlled released under acidic conditions with sustained feature. This suggests that the HAP–CSMRs might be used as the potential DDS to treat tumors with good specificity and long duration.

2. Materials and methods

For the preparation of HAP–CSMRs, aqueous solutions of CS (4.17 mg/mL, 30 mL) and $CaCl_2$ (5.55 mg/mL, 10 mL) were mixed together under stirring for 2 h. Then, $NaH_2PO_4 \cdot 2H_2O$ aqueous solution (4.67 mg/mL, 10 mL) was added dropwise under stirring. Subsequently, the reaction system was incubated for 7 d at 25 °C. Finally, the product was collected, washed, dried under vacuum and denoted as HAP–CSMRs.

The size and morphology of the HAP–CSMRs were characterized by SEM. The crystal phase of the HAP–CSMRs was determined by XRD. The CS content in the HAP–CSMRs was determined by thermogravimetry–differential scanning calorimetry (TG–DSC) analysis. Nitrogen adsorption/desorption measurements were performed to determine the SSA of the HAP–CSMRs. The pore size distribution was calculated from the desorption branch of the nitrogen isotherm curve using Barrett Joyner Halenda (BJH) method.

HAP–CSMRs were added into DOX · HCl aqueous solution and shaken for 24 h at 30°C to load the DOX · HCl. Then the sample was centrifuged, rinsed, dried and denoted as HAP–CSMRs/DOX · HCl.

* Corresponding authors. Tel.: +86 373 3325058; fax: +86 373 3328507.
E-mail addresses: guoyuming@gmail.com (Y. Guo), yanglin1819@163.com (L. Yang).

http://dx.doi.org/10.1016/j.matlet.2014.03.084
0167-577X/

To determine the loading content, the HAP–CSMRs/DOX · HCl was treated with hydrochloric acid to recover the DOX · HCl completely and the absorbance of the solution was determined by UV–vis absorption spectroscopy at 500 nm. DOX · HCl incorporation efficiency was expressed both as loading content (% w/w) and entrapment (%) represented by Eqs. (1) and (2), respectively. The reported data were the mean values of triplicate determinations.

$$\text{Loading content } (\%\, w/w) = \frac{\text{mass of DOX} \cdot \text{HCl in HAP–CSMRs/DOXHCl}}{\text{mass of HAP–CSMRs}} \times 100 \quad (1)$$

$$\text{Entrapment } (\%\, w/w) = \frac{\text{mass of DOX} \cdot \text{HCl in HAP–CSMRs/DOX} \cdot \text{HCl}}{\text{mass of DOX} \cdot \text{HCl used in formulation}} \times 100 \quad (2)$$

The HAP–CSMRs/DOX · HCl was dispersed into PBS buffer solutions with different pH values (5.0, 6.0, and 7.4). The release experiment was performed in triplicate in a thermostatic shaker. At predetermined intervals, 4 mL of the supernatant was taken and the DOX · HCl content was determined by UV–vis analysis. The same volume of fresh PBS buffer was added into the release system to top up to the original volume (10 mL).

3. Results and discussion

In this work, HAP–CSMRs were prepared through a facile one-pot method. The size and morphology of the HAP–CSMRs were determined by SEM. From the results, the HAP–CSMRs exhibit well-dispersed rod-like structure with rough surface (Fig. 1a and b). From the magnified image (Fig. 1c), the HAP–CSMRs are composed of nanoplates with thickness of about 40 nm through loose packing mode. Moreover, the obvious gap between the nanoplates suggests the presence of pores. From the size distribution analysis, the HAP–CSMRs display the narrow size distribution with average length of 3.73 ± 0.04 μm (Fig. 1d) and diameter of 1.03 ± 0.02 μm (Fig. 1d inset). Through the BET analysis, the SSA of the HAP–CSMRs is 74.45 m^2/g (Fig. 2a). In addition, the average diameter of the pores is about 16.6 nm (Fig. 2a, inset), indicating the mesoporous feature of the HAP–CSMRs.

From the XRD result (Fig. 2b), the HAP–CSMRs exhibit characteristic diffraction peaks corresponding to HAP (PDF 73-0293), revealing the successful preparation of HAP. From FT-IR measurements (Fig. 2c), compared with CS, in addition to the characteristic bands of HAP at 559, 603, 1032 cm^{-1} [16], the absorption bands of –C–O, –OH, $-(SO_3)^-$, $-COO^-$, and –N–H of the CS molecules located at 1123, 1246, 1625, and 3429 cm^{-1} are also detected in HAP–CSMRs, indicating the presence of CS. Furthermore, the positions and intensities of the absorptions of these groups change to some extent, revealing the interactions between HAP and these groups. From the TG–DSC analysis (Fig. 2d), the CS content in the HAP–CSMRs is 16.7%.

The formation process of the HAP–CSMRs was evaluated through a series of time-dependent observations. From the results, the sphere-like nanoparticles are formed after 1 d (Fig. 3a). After 3 d, the nanoparticles assemble into the smooth microrods through the oriented connection (Fig. 3b). After 5 d, the smooth surface of the microrods changes into the partly rough surface composed of nanoplates (Fig. 3c). After 7 d, the partly rough microrods change into the completely rough mesoporous microrods (Fig. 3d).

Based on the results, a possible formation mechanism is proposed (Fig. 4). Firstly, after mixing of Ca^{2+} and CS, the Ca^{2+} accumulates around the CS through the interactions between Ca^{2+} and the functional groups of CS. Secondly, the HAP–CS hybrid nanoparticles are formed after the addition of NaH_2PO_4. Thirdly, hybrid nanoparticles connect each other to form the microrods with smooth surface. Finally, the smooth surface of the microrods

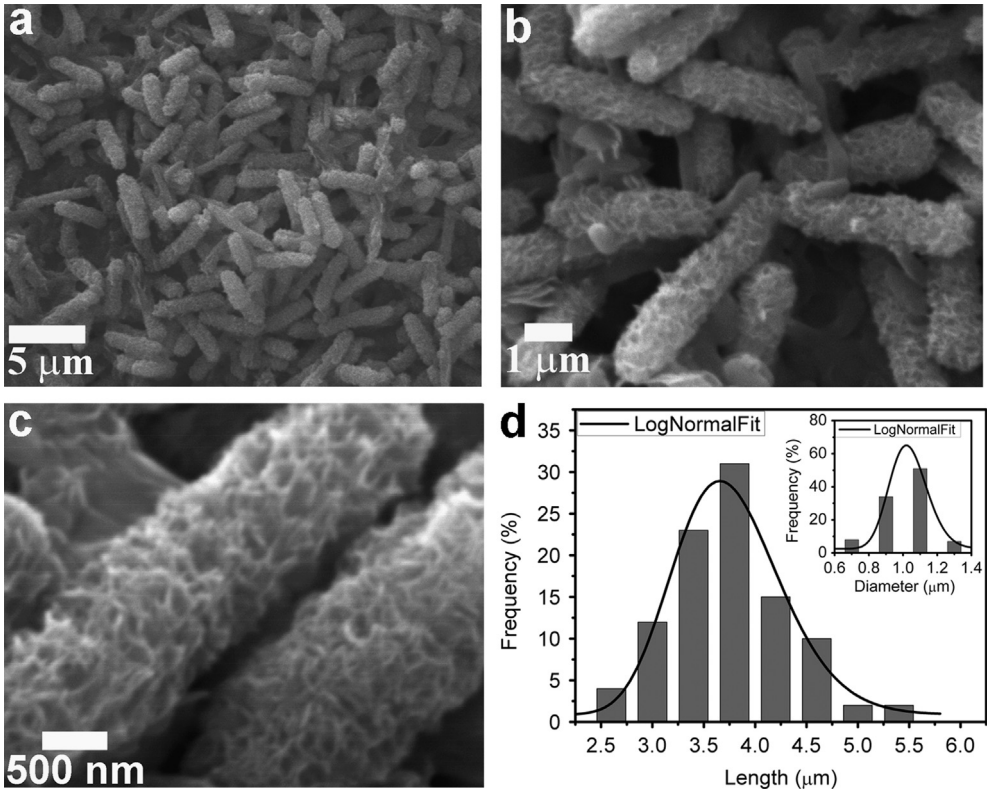

Fig. 1. (a–c) SEM images of the HAP–CSMRs with different magnifications. (d) Length distribution histogram of the HAP–CSMRs. Inset: diameter distribution histogram of the HAP–CSMRs.

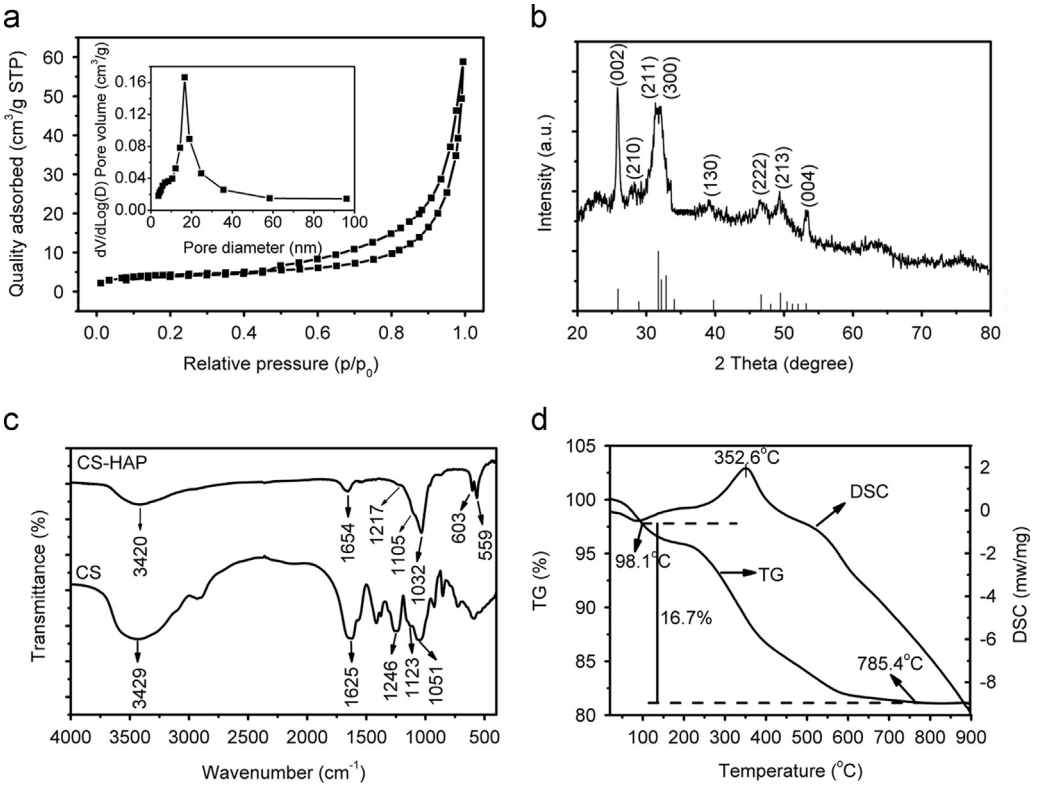

Fig. 2. (a) Nitrogen adsorption/desorption isotherm of the HAP–CSMRs. Inset: pore size distribution curve calculated from desorption branch by BJH method. (b) XRD pattern of the HAP–CSMRs. (c) FT-IR spectra of the CS and the HAP–CSMRs. (d) TG–DSC curves of the HAP–CSMRs.

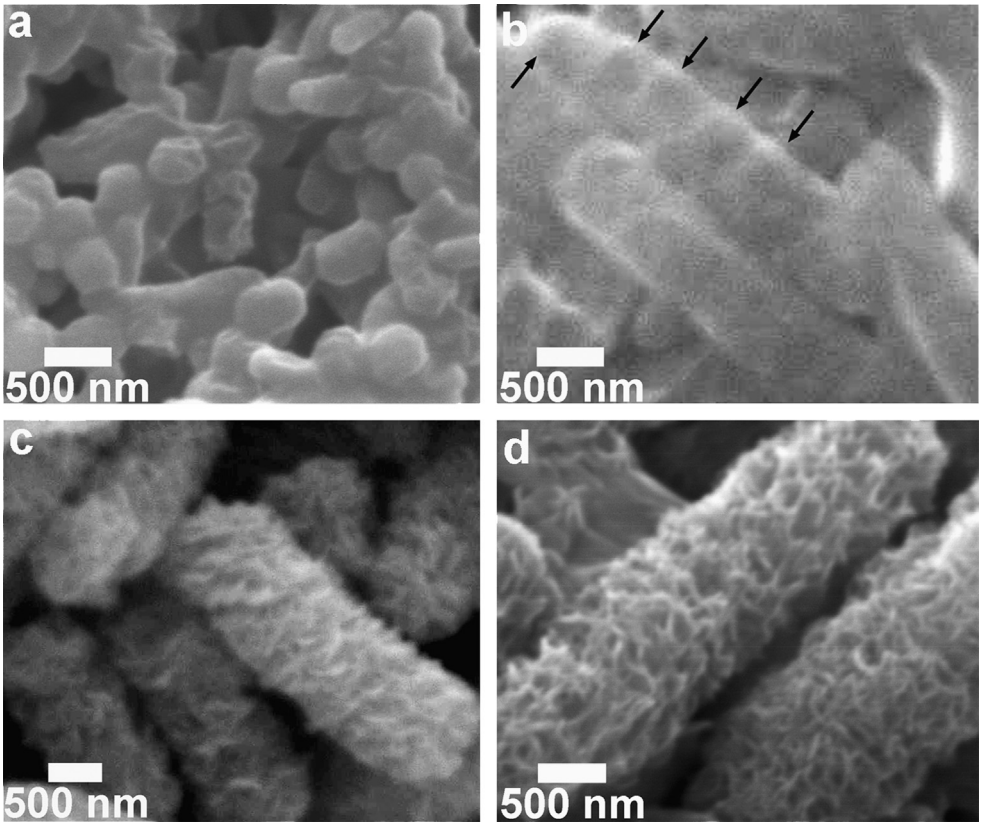

Fig. 3. SEM images of the products obtained at different reaction intervals. (a) 1 d, (b) 3 d, (c) 5 d and (d) 7 d.

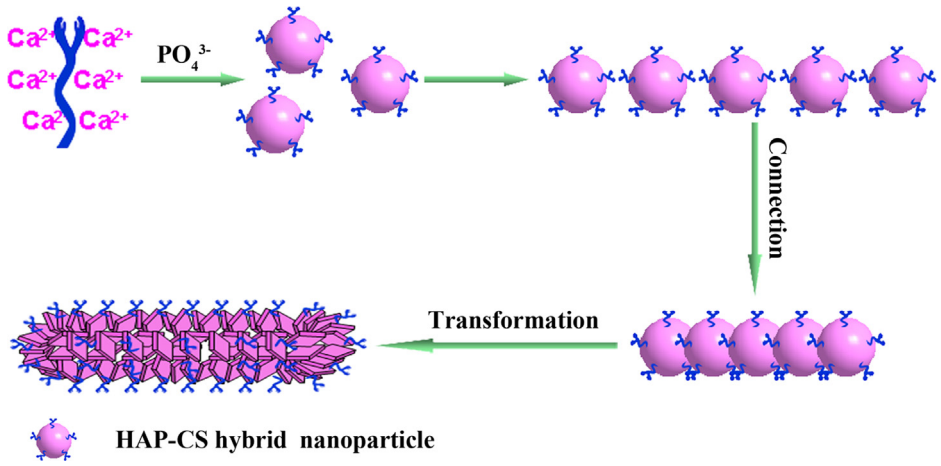

Fig. 4. Possible formation mechanism of the HAP–CSMRs.

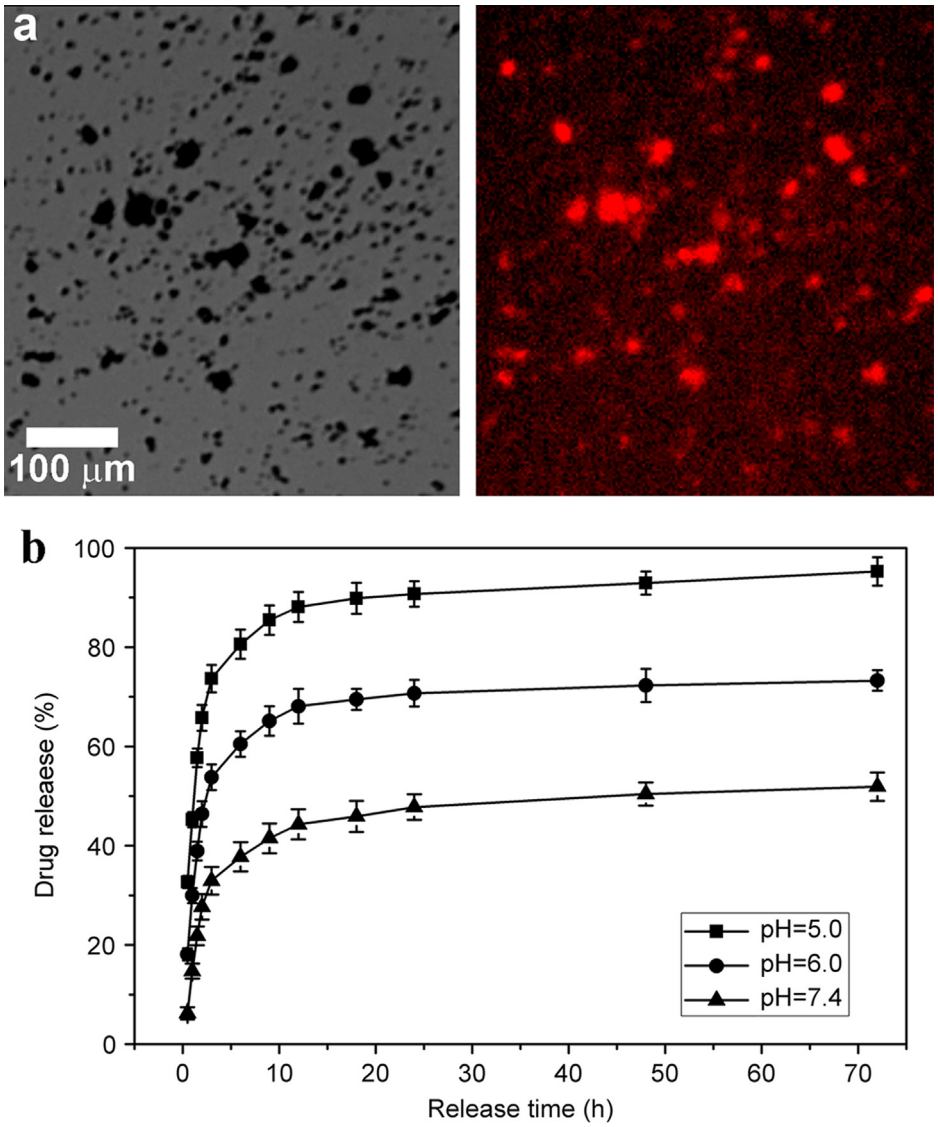

Fig. 5. (a) Light (left) and fluorescence (right) micrographs of the HAP–CSMRs/DOX · HCl. (b) *in vitro* release profiles of the HAP–CSMRs/DOX · HCl under different pH, each bar represents mean ± S.D, $n=3$.

transforms into the rough surface because of the gradual dissolution of the microrod crystals and the subsequent recrystallization process.

Using DOX · HCl as model drug, the potential application of the HAP–CSMRs as the antitumor drug carrier was studied. The loading effectiveness was evaluated with the aid of the red autofluorescence of DOX · HCl. From Fig. 5a, HAP–CSMRs/DOX · HCl emits strong red autofluorescence, indicating the successful loading of DOX · HCl. In addition, the loading content and entrapment of DOX · HCl were determined as 9.129% and 91.29%, respectively. The efficient loading can be attributed to the large SSA and mesopores of the HAP–CSMRs.

The *in vitro* release analysis showed that the HAP–CSMRs could be used as a good DDS with pH-dependent and sustained release features. From biochemical studies, the microenvironment of tumor tissues owns the lower local pH (*ca.* 5∼6) than normal tissues. This intrinsic feature can be exploited as the drug-release trigger for the pH-sensitive carriers [17]. Therefore, the *in vitro* release was performed in PBS buffers with different pH values simulating the tumor (5.0, 6.0) and normal tissues (7.4). From the results (Fig. 5b), the release efficiencies under the weak acidic conditions are much higher than that under the normal physiological condition, which can be attributed to the pH sensitivity of the HAP. This result suggests that the HAP–CSMRs might be used as a good pH-sensitive drug carrier to release the antitumor drugs to the acidic local environment of the tumor tissues. Furthermore, after initial burst release, the DOX · HCl displays the obvious sustained release profile over the period of 72 h. This can be attributed to the gradual decomposition of HAP under the weak acidic conditions. This might yield the sustained level of DOX · HCl around or inside the cancer cells to exert the cytotoxic effect for much longer duration than the pure drug, and thereby effectively enhance the antitumor effect of DOX · HCl and avoid the frequent administration.

4. Conclusions

In summary, the experimental data presented here demonstrate that CS molecules can be used as morphology-directing matrix to prepare the HAP–CSMRs with large SSA and mesopores. The features of the HAP–CSMRs, including the large SSA and mesopores, and the pH-sensitivity to the weak acidic microenvironment of the cancer cells endow them with the effective loading, controlled and sustained release of the antitumor drugs to specifically treat the tumor targets. These suggest that the as-prepared HAP–CSMRs might be used as the injectable targeted drug carrier to treat tumors with high specificity and low toxic side effect.

Acknowledgments

This work was financially supported by the National Natural Science Foundation of China (21171051, 21271066, and U1204516), the Innovation Fund for Outstanding Scholar of Henan Province (114200510004), Program for Science & Technology Innovation Talents in Universities of Henan Province (13HASTIT011), Henan Key Proposed Program for Basic and Frontier Research (112300410095) and Key Young Teachers Project of Henan Province (2012GGJS-065).

References

[1] Szakacs G, Paterson JK, Ludwig JA, Booth-Genthe C, Gottesman MM. Nat Rev Drug Discov 2006;5:219–34.
[2] Ma X, Chen H, Yang L, Wang K, Guo Y, Yuan L. Angew Chem Int Ed 2011;50:7414–7.
[3] Wang X, Cai X, Hu J, Shao N, Wang F, Zhang Q, et al. J Am Chem Soc 2013;135:9805–10.
[4] Gao PF, Zheng LL, Liang LJ, Yang XX, Li YF, Huang CZ. J Mater Chem B 2013;1:3202–8.
[5] Guo J, Hong H, Chen G, Shi S, Zheng Q, Zhang Y, et al. Biomaterials 2013;34:8323–32.
[6] Simon M, Stefan N, Plückthun A, Zangemeister-Wittke U. Expert Opin Drug Deliv 2013;10:451–68.
[7] Nicolas J, Mura S, Brambilla D, Mackiewicz N, Couvreur P. Chem Soc Rev 2013;42:1147–235.
[8] Sahoo B, Devi KSP, Banerjee R, Maiti TK, Pramanik P, Dhara D. ACS Appl Mater Interfaces 2013;5:3884–93.
[9] Tsai C-H, Vivero-Escoto JL, Slowing II, Fang IJ, Trewyn BG, Lin VSY. Biomaterials 2011;32:6234–44.
[10] Yang H-W, Hua M-Y, Liu H-L, Huang C-Y, Tsai R-Y, Lu Y-J, et al. Biomaterials 2011;32:6523–32.
[11] Muhammad F, Guo M, Qi W, Sun F, Wang A, Guo Y, et al. J Am Chem Soc 2011;133:8778–81.
[12] Schlossbauer A, Dohmen C, Schaffert D, Wagner E, Bein T. Angew Chem Int Ed 2011;50:6828–30.
[13] Guo Y, Zhang J, Jiang L, Shi X, Yang L, Fang Q, et al. Chem Commun 2012;48:10636–8.
[14] Kurapati R, Raichur AM. J Mater Chem B 2013;1:3175–84.
[15] Liang P, Liu C-J, Zhuo R-X, Cheng S-X. J Mater Chem B 2013;1:4243–50.
[16] Danilchenko SN, Kalinkevich OV, Pogorelov MV, Kalinkevich AN, Sklyar AM, Kalinichenko TG, et al. J Biomed Mater Res A 2011;96A:639–47.
[17] Stubbs M, McSheehy PMJ, Griffiths JR, Bashford CL. Mol Med Today 2000;6:15–9.